AD-A070 572 COLD REGIONS RESEARCH AND ENGINEERING LAB HANOVER NH F/G 8/12
SEA ICE RIDGING OVER THE ALASKAN CONTINENTAL SHELF,(U)
MAY 79 W B TUCKER, W F WEEKS, M D FRANK NASA ORDER-RK-8-0021
UNCLASSIFIED CRREL-79-8 NL

1 OF 1
AD A070572

END
DATE FILMED
8-79
DDC

CRREL LEVEL II

12

REPORT 79-8

ea ice ridging over the Alaskan
ontinental shelf

AD A070572

DDC
RECEIVED
JUN 29 1979
C

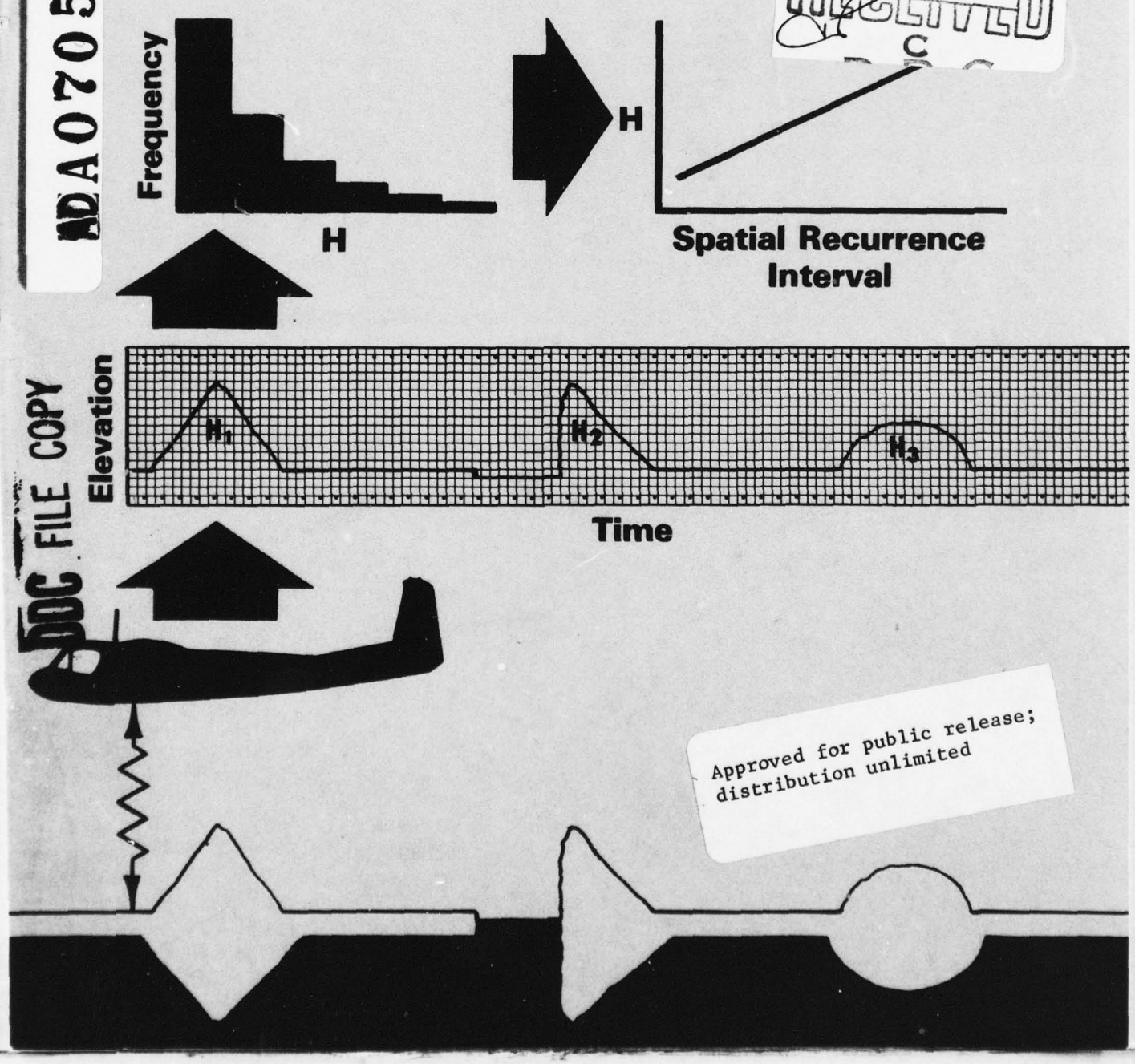

DDC FILE COPY

Approved for public release;
distribution unlimited

Unclassified
SECURITY CLASSIFICATION OF THIS PAGE *(When Data Entered)*

REPORT DOCUMENTATION PAGE

READ INSTRUCTIONS BEFORE COMPLETING FORM

1. REPORT NUMBER: CRREL Report 79-8
2. GOVT ACCESSION NO.
3. RECIPIENT'S CATALOG NUMBER
4. TITLE *(and Subtitle)*: SEA ICE RIDGING OVER THE ALASKAN CONTINENTAL SHELF
5. TYPE OF REPORT & PERIOD COVERED
6. PERFORMING ORG. REPORT NUMBER
7. AUTHOR(s): W.B. Tucker, III, W.F. Weeks and M.D. Frank
8. CONTRACT OR GRANT NUMBER(s): National Oceanic and Atmospheric Administration Order No. RK-8-0021
9. PERFORMING ORGANIZATION NAME AND ADDRESS: U.S. Army Cold Regions Research and Engineering Laboratory, Hanover, New Hampshire 03755
10. PROGRAM ELEMENT, PROJECT, TASK AREA & WORK UNIT NUMBERS: 12 31p.
11. CONTROLLING OFFICE NAME AND ADDRESS: Bureau of Land Management, Washington, D.C.
12. REPORT DATE: May 1979
13. NUMBER OF PAGES: 28
14. MONITORING AGENCY NAME & ADDRESS *(if different from Controlling Office)*: 14 CRREL-79-8
15. SECURITY CLASS. *(of this report)*: Unclassified
15a. DECLASSIFICATION/DOWNGRADING SCHEDULE
16. DISTRIBUTION STATEMENT *(of this Report)*: Approved for public release; distribution unlimited. 15 NASA Order-RK-8-0021
17. DISTRIBUTION STATEMENT *(of the abstract entered in Block 20, if different from Report)*
18. SUPPLEMENTARY NOTES
19. KEY WORDS *(Continue on reverse side if necessary and identify by block number)*
Arctic Ocean
Extreme values
Laser profilometry
Ridges
Sea ice
Statistical models
20. ABSTRACT *(Continue on reverse side if necessary and identify by block number)*

Sea ice ridging statistics obtained from a series of laser surface roughness profiles are examined. Each set of profiles consists of six 200-km-long flight tracks oriented approximately perpendicular to the coastline of the Chukchi and Beaufort Seas. The landward ends of the profiles were located at Point Lay, Wainwright, Barrow, Lonely, Cross Island and Barter Island. The flights were made in February, April, August, and December 1976, and one additional profile was obtained north of Cross Island during March 1978. It was found that although there is a systematic variation in mean ridge height ($\bar{h}$) with season (with the highest values occurring in late winter), there is no systematic spatial variation in $\bar{h}$ at a given time. The number of ridges/km (μ) is also high during the late winter, with the highest values occurring in the Barter and Cross Island profiles. In most

DD FORM 1 JAN 73 1473 EDITION OF 1 NOV 65 IS OBSOLETE
037 100
Unclassified
SECURITY CLASSIFICATION OF THIS PAGE *(When Data Entered)*

micron

Cont

profiles, the ice 20 to 60 km from the coast is more highly deformed (higher μ values) than the ice either nearer the coast or farther seaward. The Wadhams model for the distribution of ridge heights gives better agreement with observed values in the higher ridge categories than does the Hibler model. Estimates of the spatial recurrence frequency of large pressure ridges are made by using the Wadhams model and also by using an extreme value approach. In the latter, the distribution of the largest ridges per 20 km of laser track was found to be essentially normal. Wadhams' distribution consistently predicts slightly larger ridge sails than does the extreme value approach. The main factors currently limiting the accurate prediction of the temporal recurrence of large pressure ridges are limited knowledge of the drift of near-shore ice and data that would permit the assessment of year-to-year variability in μ.

microns

PREFACE

This report was prepared by W. B. Tucker, III, and Dr. W. F. Weeks, Geologists, Snow and Ice Branch, Research Division, and M. D. Frank, Electronics Technician, Alaskan Projects Office, U.S. Army Cold Regions Research and Engineering Laboratory. (During the final stages of report preparation, Dr. Weeks was the occupant of the ONR chair of Arctic Marine Science at the Department of Oceanography, Naval Postgraduate School, Monterey, California.) Funding for this study was provided by the Bureau of Land Management, through interagency agreement with the National Oceanic and Atmospheric Administration, under which a multi-year program responding to needs of petroleum development of the Alaskan continental shelf is managed by the Outer Continental Shelf Environmental Assessment Program (OCSEAP) Office. The March 1978 profiles were obtained during a NASA Lewis Research Center remote sensing experiment, and the other profiles were acquired with aircraft from the Naval Arctic Research Laboratory.

Dr. W. D. Hibler, III, and S.F. Ackley of CRREL technically reviewed the manuscript of this report.

The authors would like to thank the staffs of the National Aeronautics and Space Administration and the Naval Arctic Research Laboratory for their support. Appreciation is also expressed to S. Fungcharoen for his assistance in data analysis and to Dr. G. Weller for his overall support.

The contents of this report are not to be used for advertising or promotional purposes. Citation of brand names does not constitute an official endorsement or approval of the use of such commercial products.

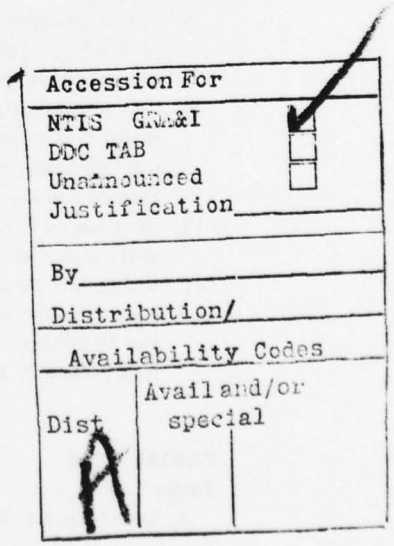

CONTENTS

	Page
Abstract	i
Preface	iii
Introduction	1
Data collection and processing	2
Analysis	3
General	3
Variations in ridging	4
Ridge height distributions	7
Occurrence of high ridges	10
The tail of the distribution	13
Extreme values	14
Applications to offshore design	15
Conclusions	17
Literature cited	18
Appendix A. Tabulated ice ridge data	19

ILLUSTRATIONS

Figure

1. Location and orientation of the laser sampling tracks . . . 2
2. Mean ridge height $\bar{h}$ as a function of distance from shore for all locations and sampling times in 1976 . . . 5
3. Number of ridges μ per 20-km interval as function of distance from shore for all locations and sampling times in 1976 . . . 5
4. μ and $\bar{h}$ values obtained in March 1978 by NASA plotted as a function of distance from shore . . . 7
5. Ridging intensity I_r as a function of distance from shore for all locations and sampling times in both 1976 and 1978 . . . 8
6. Histograms of predicted versus observed ridge heights separated into class intervals of 0.3 m . . . 9
7. Total χ^2 values for each ridge sail height class interval . . . 11
8. The Wadhams ridge height distribution function parameters α and β plotted as a function of distance from the shore of Cross Island during February, April and December 1976 . . . 11
9. The Hibler ridge height distribution function parameters N_0 and λ plotted as a function of distance from the shore of Cross Island during February, April and December 1976 . . . 12
10. Plot of $\log_{10}$ vs ridge sail height . . . 13
11. Semilog of $P_c(h)$, the probability that a ridge encountered at random will have a height of at least h meters, versus ridge sail height . . . 13
12. Ridge sail heights versus spatial recurrence intervals . . . 15
13. Monte Carlo simulation of the extreme ridge heights generated by the Wadhams and Hibler models using μ and $\bar{h}$ from the Beaufort Sea February and April tracks . . . 16

TABLES

Table

1. Least-squares constants α, β and β^{-1} . . . 14

SEA ICE RIDGING OVER THE ALASKAN CONTINENTAL SHELF

W.B. Tucker III, W.F. Weeks, and M.D. Frank

INTRODUCTION

In an attempt to assess the surface roughness of Alaskan near-shore sea ice during all seasons of the year, a series of remote sensing flights using a laser profilometer as the primary sensor were carried out in 1976. Although several studies have been made of the ridging characteristics farther offshore in the central Beaufort Sea (Hibler et al. 1974, Tucker and Westhall 1973), only Wadhams (1976) and Weeks et al. (1978) have investigated ridging in the near-shore region. Wadhams' study area was located north of the Mackenzie Delta, an area that might be expected to show significantly different ridging characteristics because of the increased width of the continental shelf there and the fact that the strong east-west motions associated with the Pacific Gyre are located farther offshore in this region. The Weeks et al. (1978) report is a preliminary analysis based on the same February 1976 laser tracks that are treated in the present study.

It is important that the degree of ridging of the near-shore sea ice off the Alaskan coast be well-characterized, inasmuch as recent field and model studies of near-shore ice motions (Weeks et al. 1977, Tucker et al. 1978, Hibler 1978, Pritchard 1978) have suggested that in the fall and early winter the impingement of heavy multiyear offshore ice along the Beaufort Sea coast commonly results in large forces stressing the fast and near-shore ice. Because this ice is thin, these stresses are usually sufficient to produce heavy ridging in both the outer reaches of the fast ice zone and within the near-shore pack ice. Supporting this expectation are visual observations made during numerous ice reconnaissance overflights indicating that the near-shore pack ice and outer portions of the fast ice along the Beaufort coast are indeed more heavily deformed than ice farther offshore. Since offshore development of oil and gas is anticipated in this coastal area in the near future, the adequate quantitative characterization of near-shore ridging is an essential step in assessing the hazards that the ice environment will pose to development and in designing ways to acceptably circumvent these hazards. Such knowledge is also required for the verification of numerical models that simulate the drift and dynamics of near-shore pack ice and the coupling between this ice and the fast ice, again subjects of considerable applied interest.

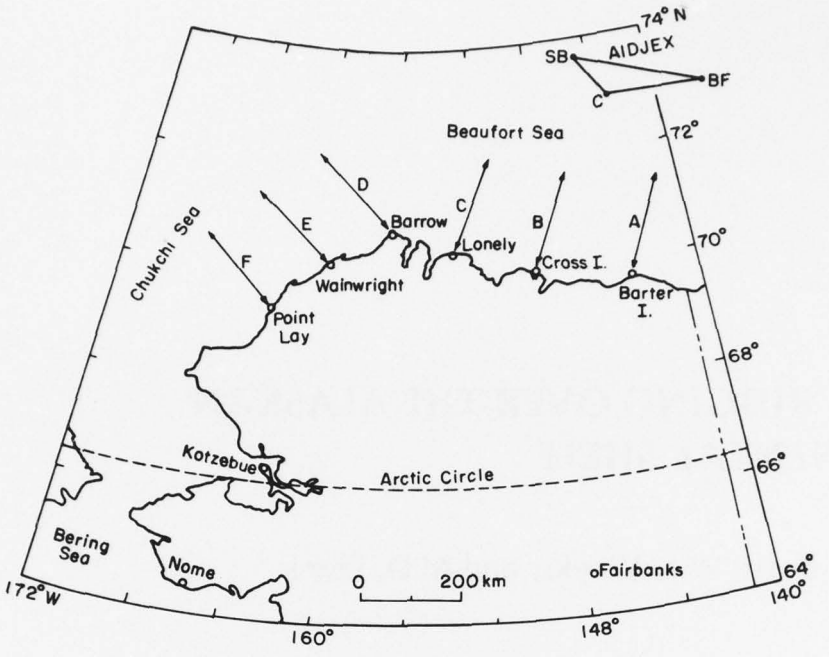

Figure 1. Location and orientation of the laser sampling tracks. The letters C, BF and SB on the AIDJEX "triangle" stand for the names of the drifting stations, Caribou, Blue Fox and Snow Bird. The positions indicated are approximate locations of the stations during February 1976.

DATA COLLECTION AND PROCESSING

Each laser flight was 200 km in length and was oriented normal to the coast. The flights proceeded into the Chukchi Sea from starting points at Point Lay, Wainwright, and Barrow and into the Beaufort Sea from Lonely, Cross Island (Prudhoe Bay), and Kaktovik (Barter Island) (see Fig. 1). It was initially planned to examine seasonal variations in the ice roughness by repeating the flights in February, April, August, and December. Due to inclement weather and the unavailability of aircraft, only the Barrow track proved usable in August. Likewise, the Lonely and Wainwright tracks are missing from the December data set, resulting in a total of 17 track lines.

The laser profiles were made by measuring the distance between the aircraft and the upper surface of the sea ice with a Spectra-Physics Geodolite 3A laser profilometer. The characteristics of this instrument have been described in several published reports (e.g. Ketchum 1971, Tooma and Tucker 1973). In the present study, ridge heights were manually catalogued from an analog strip chart recording of the ice surface profile. The heights of the ridges were taken as the vertical distances above a curve representing the altitude variations of the aircraft. Ridges were discriminated using the Rayleigh criterion as applied by Lowery (1975), which classifies an independent ridge as having at least twice the elevation as the shallowest troughs on either side. This criterion prevents the sidelobes of large ridges from being included in the ridge counts. The minimum ridge height considered in our study was 0.9 m (3 ft). Ridges were further categorized into 0.3-m (1-ft) height class intervals and the number of ridges per 20 km of track was recorded (Table AI presents a data tabulation). The 20-km interval was believed to be small enough to resolve spatial variations within the near-shore region while still containing enough ridges to provide a statistically reliable sample.

ANALYSIS

General

In studies of the intensity and distribution of pressure ridging, the ridge heights obtained from the laser profiles are usually tabulated into frequency distributions that are taken to be representative of the region sampled. Comparisons are then made between statistics computed from these sample distributions in order to estimate spatial and temporal changes in the parent distributions. Of particular interest to engineers contemplating design problems related to offshore development is the probability of occurrence of particularly high ridges—ridges sufficiently rare that their occurrence in the limited set of any specific sample is unlikely. In making estimates of the probability of such rare events, the choice of the form of the assumed parent distribution to be fitted to the sample data is of considerable importance.

In past studies two different ridge height distributions have commonly been used. The first of these was developed by Hibler et al. (1972) to fit distributions of pressure ridge keel depths and was also found to work well for ridge sails. The distribution was derived by a variational calculation based on two fundamental assumptions concerning the nature of ridges: first, that all ridge height arrangements yielding the same net deformation are equally likely, and second, that all ridge cross sections are similar in a geometric sense. Specifically, it was assumed that the cross-sectional areas of all ridges are proportional to the square of the ridge height times a constant proportionality factor. The resulting distribution gives the number of ridges occurring between a specified height h and $h+dh$ as

$$n(h)\,dh = N_0 e^{-\lambda h^2} dh \tag{1}$$

where

$$N_0 = 2\mu\lambda\bar{h}e^{\lambda h_0^2} \tag{2}$$

and λ is a parameter determined by iteration from

$$e^{-\lambda h_0^2} = \bar{h}(\lambda\pi)^{1/2}\,\mathrm{erfc}\,\lambda^{1/2}h_0. \tag{3}$$

Here, h_0 is the minimum ridge height considered, $\bar{h}$ is the mean ridge height for the section, μ is the number of ridge elevations above h_0 per unit distance and erfc is the complementary error function. This model has been successfully tested on many sets of ridge height data spanning a period of several years (Hibler et al. 1974).

Wadhams (1976, 1978), on the other hand, empirically chose a distribution of the form

$$n(h)\,dh = \alpha e^{-\beta h} dh \tag{4}$$

where $n(h)$ is again the number of ridge heights occurring between h and $h+dh$ and α and β are analytically determined from

$$\beta = (\bar{h} - h_0)^{-1} \tag{5}$$

and

$$\alpha = \mu\beta e^{\beta h_0}. \tag{6}$$

His reasons for using this distribution were that it is computationally simpler (no iterative solution required) and it appeared to fit his data on higher ridges better than the Hibler model. However, it should be noted that eq 4 is a special case of the Hibler model if ridges are assumed to be rectangular in cross section. In the following, we will fit both types of distributions to our data in order to compare their usefulness to the region of the Beaufort Sea where offshore development is imminent.

We will also investigate the intensity of the ridging as a function of location and season. In the past, ridging intensity γ has been described by the parameter

$$\gamma = \mu/\lambda \tag{7}$$

where μ is the number of ridges above a specified minimum height per given length of track and λ the distribution shape parameter from the Hibler ridge height distribution (eq 3). This is a useful parameter in that it has units of length^2/length (m^2/km) and can be used as an index of the volume of deformed ice along the sampling track (Hibler et al. 1974). In the following we will not use γ because it is conceptually tied to the Hibler distribution function. Instead we will use a simple function also initially suggested by Hibler et al. (1974):

$$I_r = \mu(\bar{h})^2 \cot\theta \tag{8}$$

where $\bar{h}$ is the mean ridge height (above a specified cutoff) and θ is the assumed ridge slope angle. I_r, the area of deformed ice under the laser path, is therefore proportional to the topside volume of ice along the laser track and has units identical to γ. As pointed out by Hibler et al. (1974), if the ridges along the sampling track are randomly oriented, then the volume of deformed ice per unit area above water level can simply be obtained from the product $(\pi/2)I_r$. An estimate of the effective ice thickness due to the total volume of deformed ice per unit area in ridges is $10(\pi/2)I_r$ which assumes that there is 9 times as much ice in the keels as in the sails. Actual sail slopes measured normal to the axes of ridges average about 25° for first-year ridges. Our assumption that $\theta = 18.43°$ is a conservative estimate in that it overestimates the amount of ice in the sails. Also because laser profiles cross ridges at a variety of angles, the average sail slope measured by laser is less than that determined by detailed "on-site" profiles.

Variations in ridging

In examining the variability of ridging with location and season, we first will study the variability of μ and $\bar{h}$, the parameters that combine to form I_r. Figure 2 shows plots of $\bar{h}$ for each 20-km interval vs distance from shore for the different sample locations (the tabulated data are presented in Table AII). The $\bar{h}$ values for summer (August) and early winter (December) are low, averaging 1.21 m (4 ft). This seems reasonable inasmuch as the first-year ice which predominates in the region sampled is still relatively thin, even in December, and there are theoretical reasons to expect thinner ice to yield lower ridges when deformed (Parmerter and Coon 1972). In sharp contrast, only 3.6% of the February and April values were below 1.21 m, the mean for August and December. The February and April $\bar{h}$ values averaged 1.58 and 1.42 m, respectively, with the highest $\bar{h}$ value being 1.79 m. There is no obvious correlation between the variation of $\bar{h}$ and the distance from shore. There is also no pronounced variation in $\bar{h}$ as one moves along the coast. The one possible exception to this statement is the westernmost station, Point Lay, where in both February and April the observed $\bar{h}$ values are low. Whether or not this is a consistent pattern will require further observation. However, even considering the low $\bar{h}$ values at Point Lay, the average values of $\bar{h}$ for the Chukchi and Beaufort Seas are identical with $\bar{h} = 1.50$ m when the February and April data are combined.

The number of ridges per km (μ) vs distance from shore is plotted in Figure 3 and tabulated in Table AII. The average μ values are lower in the summer and early winter (2.73 in August based on a sample at Barrow only and 1.40 in December) and increase in February and April to values of 4.35 and 4.49 respectively. Again, this trend is conceptually reasonable, as we would expect more pressure ridges to be present later in the ice year. In thinking about the data presented in this report, one must remember that December 1976 is the start of the 1976-1977 ice year while February and April 1976 are in the 1975-76 ice year. The low μ value observed in December 1976 is supported by our visual observations (Tucker et al. 1978) made in March–May 1977 that the ice within 40 km offshore of the barrier islands north of Prudhoe Bay was noticeably less deformed in the late winter and spring 1977 than it was at a similar time in 1976.

When one examines the variations in μ along the coast in December, no appreciable difference between the ice ridging in the Beaufort and Chukchi Seas is found. In February and April, however, there are significant differences with considerably more ridges being present in the Beaufort Sea. This is reasonable in that the ice motion along the Beaufort coast is generally thought to be more convergent than the ice motion in the Chukchi Sea. The Barter Island tracks contain the most ridges, followed by those from Cross Island and from Lonely as one moves farther west. In April, all the tracks in the Chukchi Sea had fewer ridges. The same was true in February with the exception of Point Lay whose μ value (4.38 ridges/km) fell between the values observed at Cross Island and at Lonely (3.10 and 3.70 ridges/km respectively).

When the variation in μ values normal to the coast is examined, it is commonly found that the largest μ values occur at 20 to 60 km off the coast and that the ice between 20 and 100 km off the coast generally contains more ridges than the ice either closer to the coast or farther out to sea. This gives support, from the viewpoint of ice morphology and ice deformation, for considering the coastal marginal ice zone to be a separate ice province (Weeks et al. 1971, Kovacs and Mellor 1974). Laser profiles obtained in February 1976 from the Blue Fox-Snow Bird line

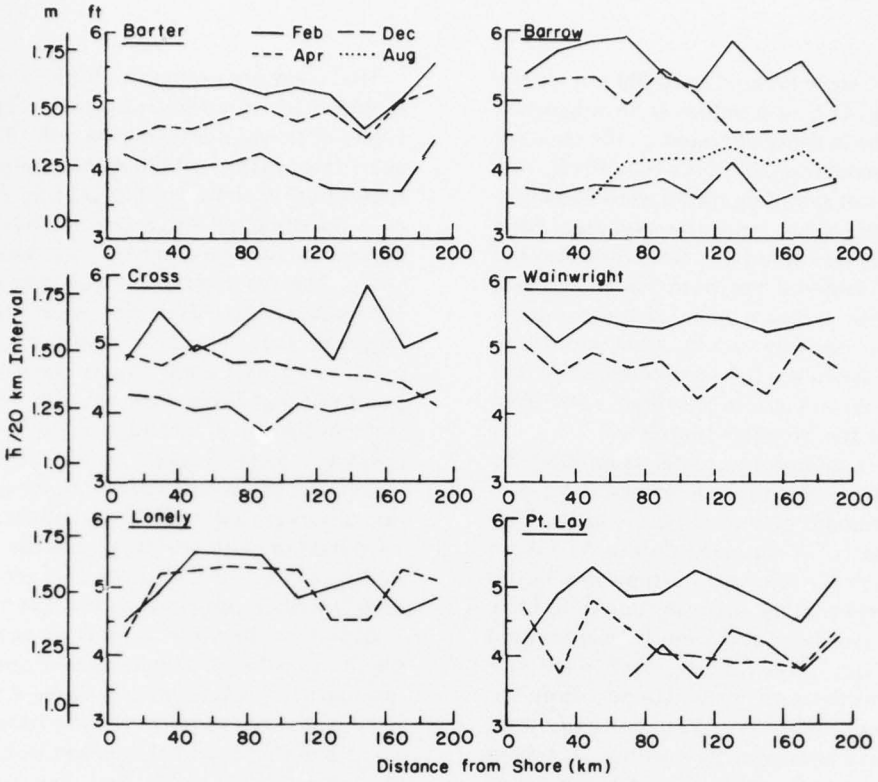

Figure 2. Mean ridge height $\bar{h}$ as a function of distance from shore for all locations and sampling times in 1976. $\bar{h}$ is computed for each 20-km interval and plotted at the center of each interval.

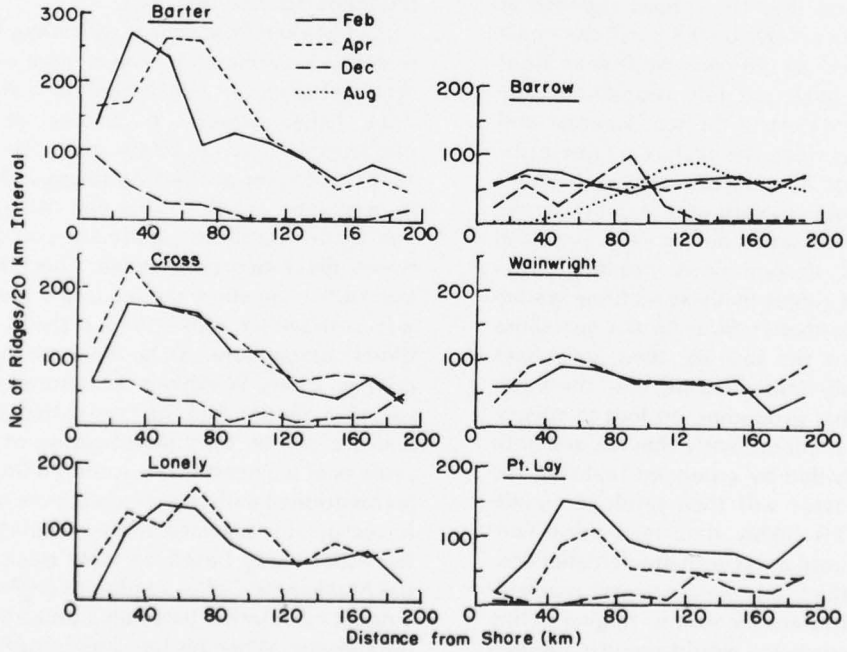

Figure 3. Number of ridges μ per 20-km interval as function of distance from shore for all locations and sampling times in 1976. Values are plottted at the center of the sampling interval.

of the AIDJEX array located over 400 km off the coast (see Fig. 1) give μ values (2.56 ridges/km) that are similar to those obtained on the seaward end of the coastal tracks (Weeks et al. 1978). This suggests that our sampling tracks were apparently long enough to encompass the complete zone of more highly deformed ice. Note also that the values of μ observed are both lower and less variable on the seaward ends of the sampling lines. This presumably results from more uniform stresses when the ice considered is located a reasonable distance from the shore, away from the effects of the irregular shoreline.

The above conclusions are also supported by the results of Wadhams and Horne (1978) who analyzed submarine sonar observations collected by the *U.S.S. Gurnard* during 7-10 April 1976. Although the *Gurnard's* sample tracks did not correspond exactly either in time or in location to our laser lines and were largely located seaward of our observations, data were collected on a north-south line with a nearshore termination at approximately 55 km north of Barter Island and on an east-west line with a near-shore termination approximately 170 km northeast of Barrow. In both cases the ice nearest the coast was found to be significantly more deformed than the ice farther seaward.

The observation that the largest number of ridges usually occurs 20 to 60 km off the coast can be explained as follows. Multiyear floes from the main pack are left stranded in the shallow coastal waters in the late summer and early fall at times when the pack is in close proximity to the coast. These grounded "inclusions" provide additional strength and stability to the newly forming ice sheet during freezeup, and relatively small deformations produce additional grounded ridges in these shallow waters which provide further stability to the nearshore ice. The edge of the fast ice then progresses seaward with only limited ridging until the water depth is such that grounding no longer occurs. Still containing predominantly thin ice and with no stability provided by grounded features, deformational stresses will then produce significant ridging. This highly deformed zone continues seaward until areas with much higher concentrations of thick multiyear ice are reached. Because an equivalent amount of ridging in this thicker and stronger ice would require appreciably higher stresses, the amount of ridging occurring decreases.

That there are exceptions to the above pattern is shown by an additional laser track off Cross Island obtained during mid-March 1978, nearly 2 years later than the 1976 April profiles. Figure 4 shows both $\bar{h}$ and μ for this profile, also plotted as a function of distance off the coast. The highest values of μ and $\bar{h}$ occur immediately offshore. The laser data are supported by visual observations that there was severe ridging with large ridge sails in excess of 10 m located 0.3 km north of Cross Island. Visual observations also point out that there were virtually no multiyear floes in this area, although many were seen in previous years (Tucker et al. 1978). In fact, significant concentrations of multiyear ice were not observed until 150 km offshore during the 1978 mission. Our feeling is that the absence of multiyear floes allowed the thin ice to deform very heavily quite close to the coast.

Based on our observations of near-shore ice pileups, we believe that such occurrences are not particularly rare and that they are most likely to occur at exposed offshore islands such as Cross and Barter and at exposed headlands such as Barrow. We also suggest that such coastal pileups primarily occur in years when the pack ice retreats a significant distance from the coast during the prior summer and does not move near the coast prior to freezeup.

Past workers have reported finding linear correlations between either the number of ridges or the areal amount of deformed ice and the mean ridge height based on studies using aerial photography (Gonin 1960), sonar (Hibler et al. 1972), and laser profiles (Wadhams 1976, 1978). As might be guessed from our discussion of μ and $\bar{h}$, we found no significant correlation between these two parameters. There have been two studies in which the ice under investigation was sufficiently close to our study area that direct comparisons can be made. In the more recent of these, Wadhams and Horne (1978) obtained a similar lack of correlation between μ and $\bar{h}$ based on their investigation of the sonar profiles of ice keels in the southern Beaufort Sea (as mentioned earlier, their data were largely collected at sites seaward of our sampling lines). In the other study based on laser tracks north of the Mackenzie Delta, Wadhams (1976) reported a linear correlation between μ and $\bar{h}$ but only in the summer. When his late winter (April) data are examined, however, the correlation appears curvilinear and the relation is not well defined. He

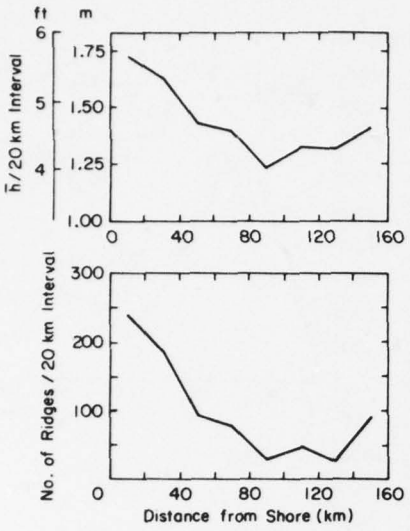

Figure 4. μ and $\bar{h}$ values obtained in March 1978 by NASA plotted as a function of distance from shore. Values are computed for each 20-km sampling interval and plotted at the center of the interval.

also did not report an area of severe ridging off the coast such as we and Wadhams and Horne (1978) observed.

Why the correlation between μ and $\bar{h}$ is absent in these data sets is not clear to us. We initially thought that the presence of large rubble fields, which appear to be particularly common near the coast, might result in unusually large numbers of small ridges (as sensed by the laser system) which would tend to obscure the relation between μ and $\bar{h}$. However, most of the area sampled by Wadhams and Horne (1978) would appear to be far enough off the coast to be outside the area of pronounced ridge and rubble formation and the correlation between μ and $\bar{h}$ is still missing. The resolution of these questions will presumably have to await the collection of more complete sets of laser and sonar observations of ridging.

Figure 5 shows the variations in the ridging intensity I_r as a function of the distance from shore. A scale giving the increase in the effective thickness of the ice due to the volume of deformed ice per unit area is also presented in Figure 5. As might be expected from the nature of the variations in $\bar{h}$ and μ, the I_r patterns agree with the patterns suggested by μ. In February and April the highest I_r values occur from 20 to 60 km off the coast, and the ice between 20 and 100 km off the coast was more highly deformed than the ice nearest the coast or the ice farther out to sea. The data from the 1978 Cross Island traverse are also plotted in Figure 5, and as with μ in Figure 4, the largest I_r value occurs in the 20-km section closest to the coast. These results are similar to the ridging patterns found by Hibler and Ackley (1973) who also suggested that there was a band of more highly deformed ice along the north coast of Alaska. However, present information suggests that this ice is appreciably less deformed than the near-coastal ice found off the north coasts of the Canadian Archipelago and Greenland.

It should be mentioned that the μ values reported in the present report, when determined as the number of ridges per kilometer that are greater than 1.22 m (4 ft) in height, agree favorably with values (1.15 to 4.2) reported from the same general region by Hibler et al. (1974). Our northernmost μ and $\bar{h}$ values are also in good agreement with those reported by Wadhams (1976) for locations 150 to 200 km north of the Mackenzie Delta in April 1975. However, Wadhams observed a steady decrease in μ as he approached the coast, and as mentioned earlier, there was no evidence of a band of more highly deformed ice. While we believe that this lack of a pronounced zone of intense ridging may be the rule rather than the exception in the Mackenzie Delta region, we still cannot rule out the possibility of the differences being attributed to yearly variations.

Ridge height distributions

Now that we have some general sense of the spatial and temporal patterns of the ridging off the north coast of Alaska, we will examine the general form of the observed sail height distribution and then the expected frequency of encounters with very large ridges.

Figure 6 shows a histogram of the ridge sail frequencies compiled for the complete 200-km sampling tracks from Barrow for the different seasons. Also given in Figure 6 are the expected frequencies of each height class interval using the Hibler and Wadhams distributions.

A more quantitative examination of the degree of fit to the data of the different models can be made using a χ^2 test. For the total sampling tracks (18, including the March 1978 track),

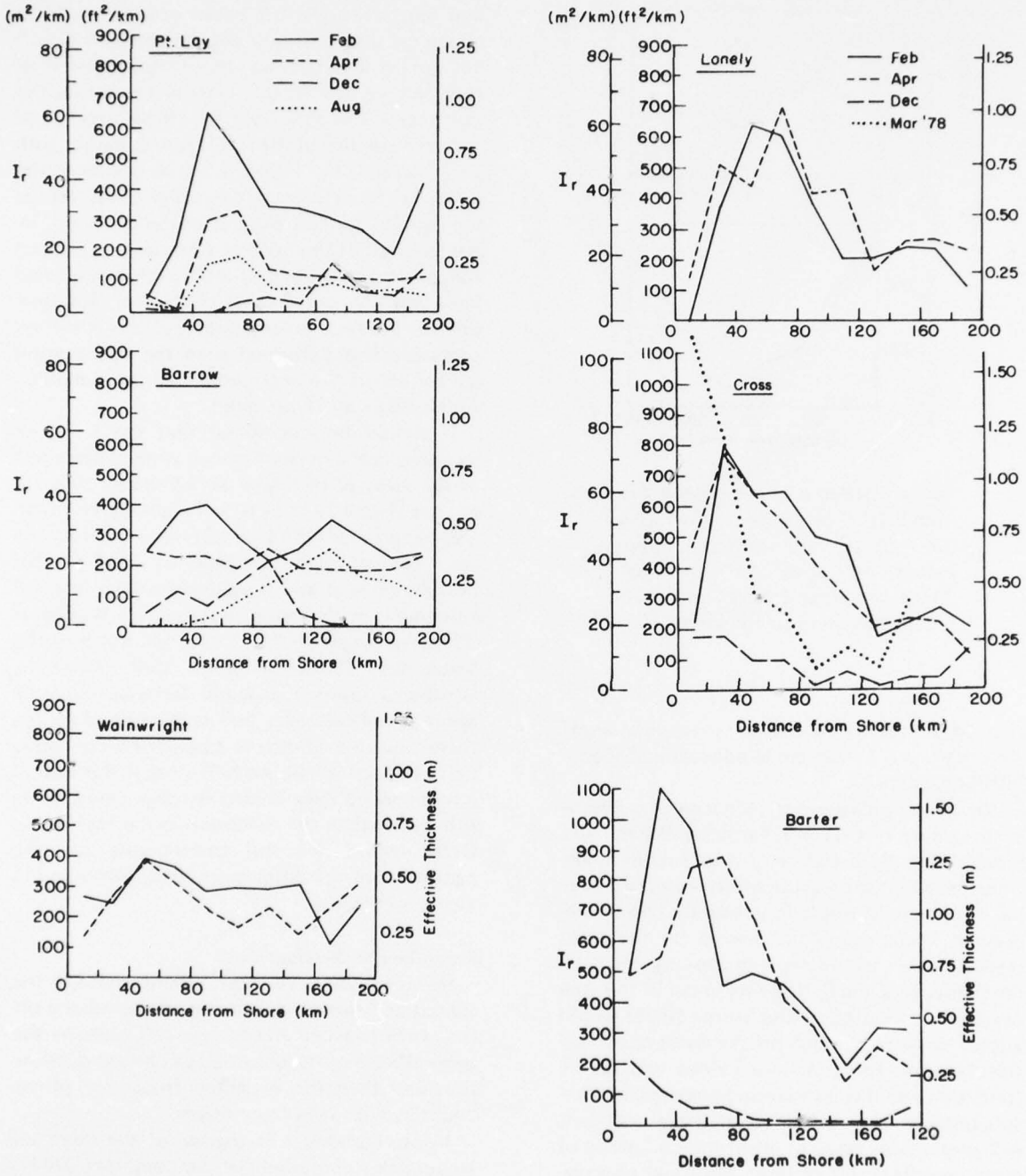

Figure 5. Ridging intensity I, as a function of distance from shore for all locations and sampling times in both 1976 (Feb, Apr, Aug, Dec) and 1978 (Mar). Values are computed for each 20-km sampling interval and plotted at the center of the interval. The effective thickness is that due to the volume of deformed ice per unit area.

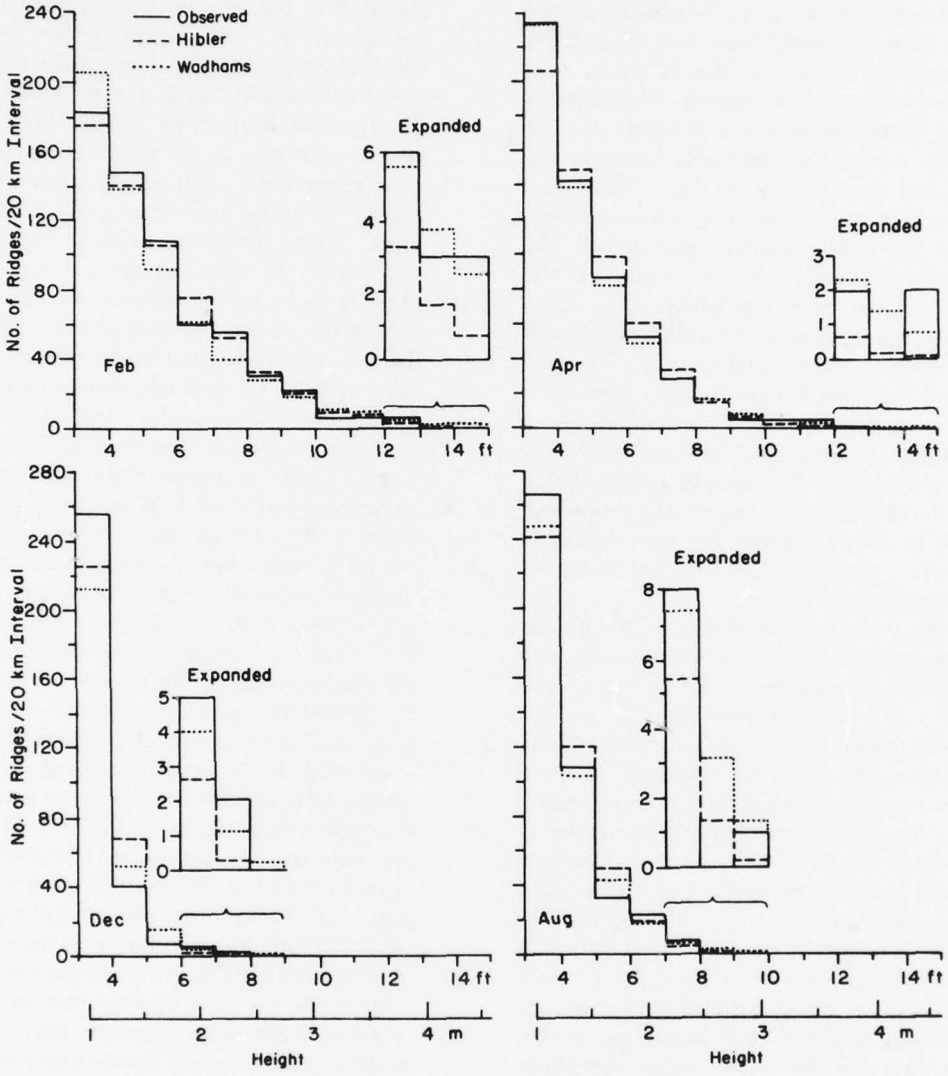

Figure 6. Histograms of predicted versus observed ridge heights separated into class intervals of 0.3 m (1 ft). The samples are from Barrow on February, April, August, and December 1976 and are based on the complete 200-km sampling tracks. The fitted distribution functions are described in the text.

the Wadhams model predictions all pass the χ^2 test at the 0.05 level. The Hibler model predictions pass in all but one case (the Barter Island February track). However, the Wadhams model has lower (more acceptable) χ^2 values than the Hibler model in 15 out of the 18 cases considered. As can be seen in Figure 6, the Wadhams model is in better agreement with the data in the higher ridge categories, primarily because the Hibler model consistently predicts fewer high ridges than observed. Higher χ^2 values are obtained for the Hibler model inasmuch as the divisor in calculating the χ^2 value is the predicted number of ridges which is, in some cases, a very small number. This is demonstrated in Figure 7 which shows total χ^2 values for each given ridge sail height class interval (the data used are from the February Cross Island track). The χ^2 values are similar up to ridge heights of approximately 3 m (9 ft), indicating little choice between the two distributions. However, at large ridge heights the χ^2 values for the individual class intervals are significantly larger when the Hibler distribution is used.

When the data are considered in 20-km sections as opposed to complete 200-km tracks, the fits of both models improve. The reason for the improvements is that, as was discussed earlier, the 200-km tracks are not usually statistically homogeneous, showing significant spatial variation in the number of ridges encountered. Again the fits of the Wadhams distribution passed at the 0.05 level on all 174 of the 20-km sample tracks used (some of the individual 20-km intervals were unusable). The Hibler distribution was less successful, with 10 of the 174 fits failing at the 0.05 level. However, the overall results were similar to those achieved with the 200-km tracks: the Wadhams relation gave better agreement with the data for the higher ridge categories while both models appeared adequate for the lower and medium height classes.

Figures 8 and 9 show, respectively, the constants α and β of the Wadhams model and N_0 and λ of the Hibler model determined for the different 20-km sections of the Cross Island tracks for February, April, and December 1976. The constants for the other tracks show similar variations and are listed in Table AIII. It is not uncommon for α and N_0 to vary by a factor of 10 from one sampling section to another. The values of β and λ vary by a factor of up to 5. The only pattern discernible to us in these coefficients is that, as expected, the variations in α and N_0 are similar to the previously discussed variations in μ.

In past studies of ridging it has been generally found that the Wadhams distribution is more successful on ridge sails, while the Hibler distribution is more successful on ridge keels. Sails are sampled with a narrow-beam sensor (laser) while keels have usually been sampled with a wide-beam sensor (sonar). However, recent sonar data obtained with a narrow-beam system are fitted better by the Wadhams distribution. These observations have led Wadhams and Horne (1978) to advance a hypothesis explaining the varying degrees of success of the two distributions. The Hibler theory is built on the concept of geometrically congruent ridges, each with the same shape possessing a mass and a potential energy which depend only on the keel depth (or sail height). Wide-beam sensors force ridges to approximate this concept by smoothing out their fine structure and leaving them as discrete entities. Narrow-beam sounders, on the other hand, see the holes and hollows in ridges and tend to split large ridges into multiple "ridges." If the Wadhams and Horne hypothesis is correct, it replaces the question of which distribution is correct (both are "correct" in their place) with the question of which distribution is most applicable to the particular problem under discussion. If we were discussing the potential energy associated with ridging, we would opt for the Hibler distribution. In the present report we are, of course, primarily interested in the hazards posed to offshore development by the presence of ridges. For this problem we suggest that the Wadhams distribution is the more useful in that it will tend to overestimate the number of large ridges (i.e. it contains a built-in safety factor) and these ridge segments may well act as discrete entities when ice-structure interactions are considered.

Occurrence of high ridges

Because of the increased probability of offshore construction in the waters of the Chukchi and (particularly) Beaufort Seas, there is considerable interest in predicting the number of large pressure ridges that might impact an offshore structure as a function of time. In most cases, however, the ridges of interest are sufficiently rare that they may not be represented in the sample of ridges upon which the prediction is to be based. There are two common ways to

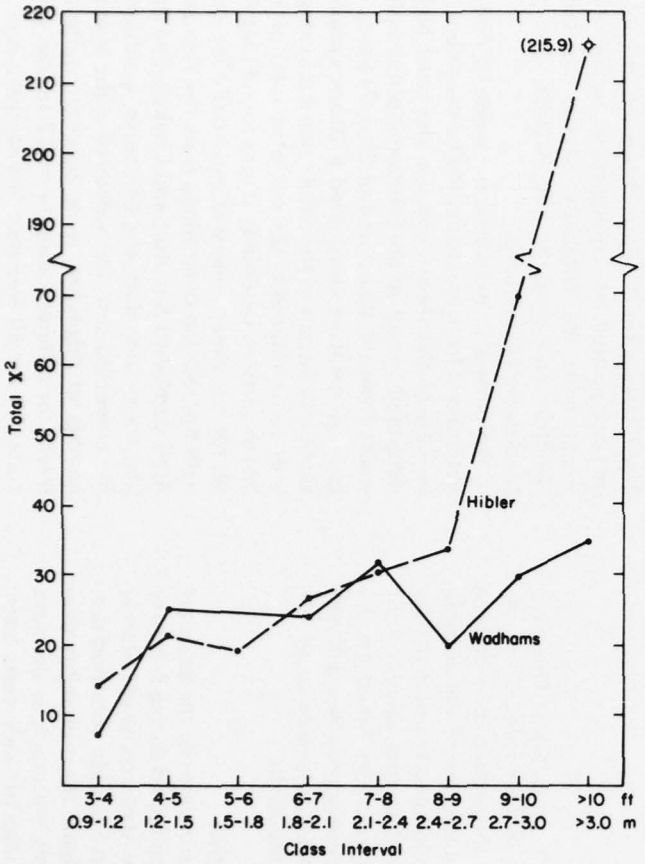

Figure 7. Total χ^2 values for each ridge sail height class interval. The data used are from the February 1976 Cross Island track.

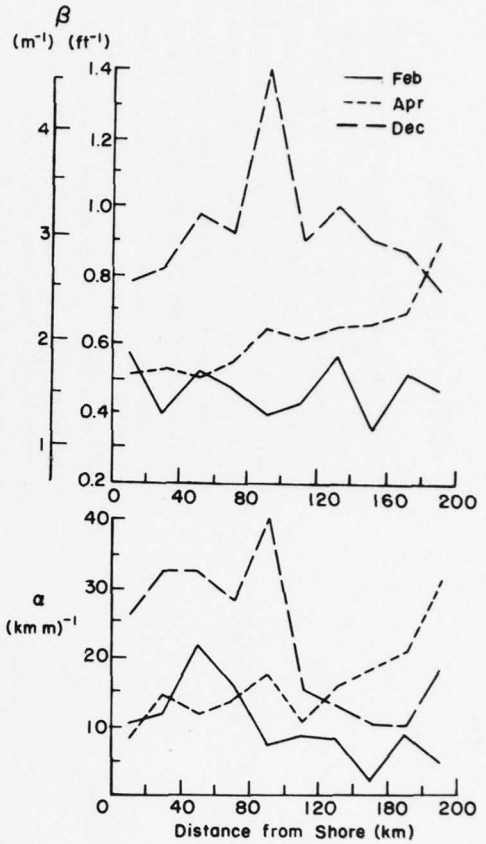

Figure 8. The Wadhams ridge height distribution function parameters α and β plotted as a function of distance from the shore of Cross Island during February, April, and December 1976. Values are computed for each 20-km interval and plotted at the center of the interval.

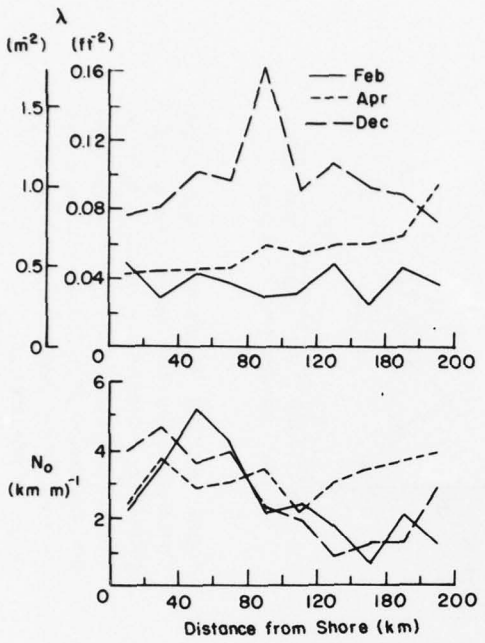

Figure 9. The Hibler ridge height distribution function parameters N_0 and λ plotted as a function of distance from the shore of Cross Island during February, April, and December 1976. Values are computed for each 20-km interval and plotted at the center of the interval.

go about making such predictions. One way would be to fit a distribution function to the data and then examine the probabilities of large ridges as given by the upper tail of the distribution. A second way would be to examine the distribution of large ridges (extreme values) in the data set and to make estimates based on this distribution. Both of these approaches will now be examined and applied to problems of offshore development in the Arctic.

The tail of the distribution

Figure 10 shows linearizations of the Beaufort and Chukchi Sea data collected during February and April, the Barrow data collected during August and the Beaufort Sea data collected during December. In the figure the probability density is per foot (0.305 m), inasmuch as the data were initially grouped into 1-ft-wide class intervals (for details see Wadhams 1976). As can be seen, each set of data collected at a given time during the ice season can be well-approximated by a straight line. The least-squares straight lines expressed in the form

$$P(h)\,dh = \alpha \exp(-\beta h)\,dh \qquad (9)$$

are given in Table 1 and shown in Figure 10. Here $P(h)\,dh$ is the probability that a ridge encountered at random will have a height in the range h to $(h+dh)$ given that its height is greater than 1 m. Also shown in Figure 10 are the least-squares lines determined from the traverse between the Blue Fox and Snow Bird stations of the AIDJEX array (Feb. 1976; Weeks et al. 1978) and the results of Wadhams' sampling of sail heights off the Mackenzie Delta region. Note that the combined (Feb.–Apr.) Beaufort and Chukchi Sea, the Mackenzie, and the AIDJEX data sets result in very similar relations when presented in this manner even though there are appreciable differences in the number of ridges between the different sampled regions.

If it is assumed that these linear relations can be extrapolated to very large sail heights, then $P_c(h)$ which is the probability that a ridge encountered at random will have a height of at least h meters, is given by

$$P_c(h) = \beta^{-1}[\alpha \exp(-\beta h)] = \beta^{-1}P(h). \qquad (10)$$

The relations for $P_c(h)$ are also given in Table 1 and are plotted on semilog paper in Figure 11. Again note the similarity of the combined Beaufort and Chukchi, the AIDJEX, and the Mackenzie Delta curves.

We have also examined the value of $P(h)\,dh$ determined from ice that could be considered to be part of the shear zone (i.e. the most highly deformed portion of the February-April sampling tracks from the Beaufort and Chukchi Seas). Arbitrarily we have considered a 20-km sampling section to be part of the shear zone if it averaged 6 or more ridges/km (23 out of a total of 120 20-km sections qualified). It was found that $P(h)\,dh$ for the shear zone was essentially identical with the relation determined from the February-April combined Beaufort and Chukchi Sea data (the shear zone data are, of course, a subset of the combined set). The values of μ, the average number of ridges/km, were, however, quite different for different areas ($\mu = 8.7$ for the shear zone, 5.5 for all Beaufort Sea samples, and 3.3 for all samples from the Chukchi Sea).

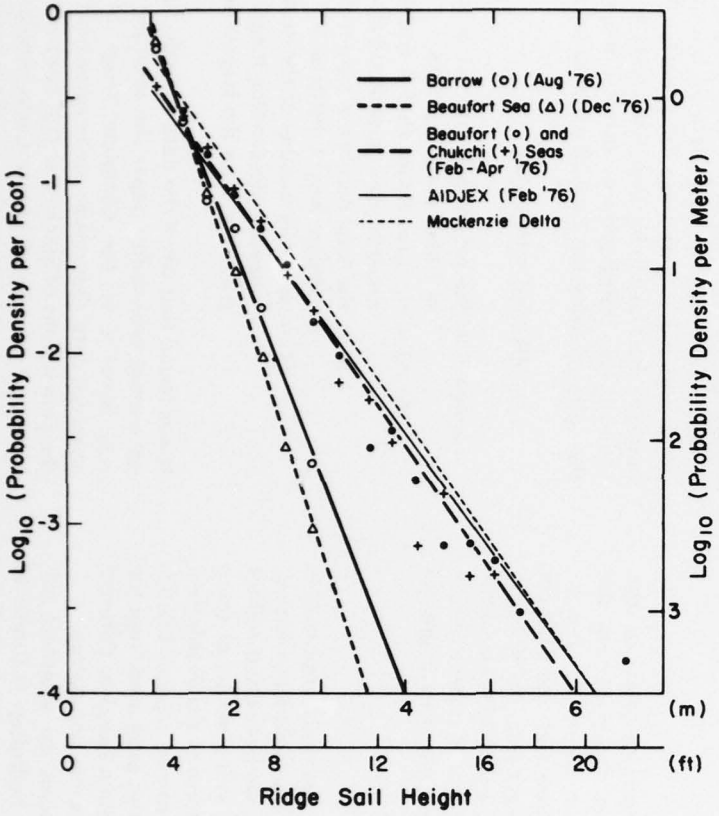

Figure 10. Plot of log $_{10}$ [probability density per foot (0.305 m)] vs ridge sail height.

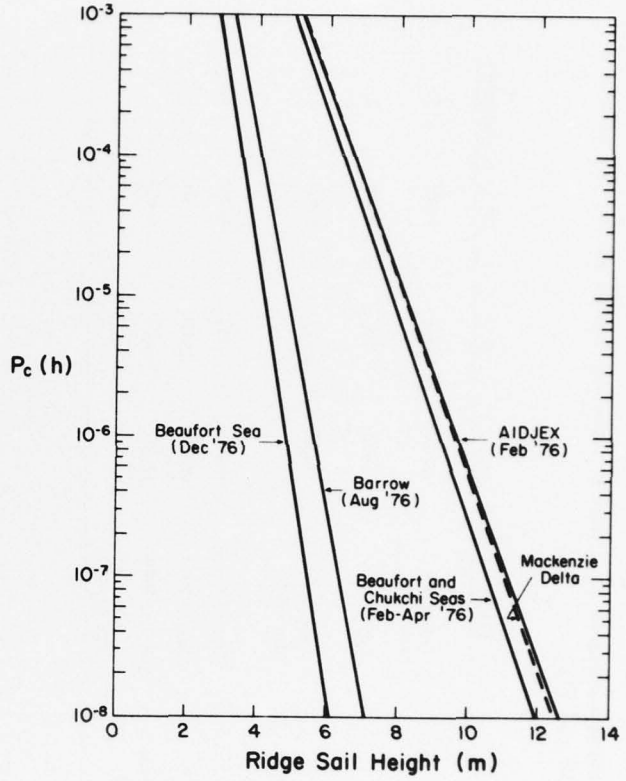

Figure 11. Semilog of P_c(h), the probability that a ridge encountered at random will have a height of at least h meters, versus ridge sail height.

Table 1. Least-squares constants α, β and β^{-1} (see eq 9 and 10 for the relations presented in Fig. 10 and 11).

Source of data	Time	α	β	β^{-1}	μ (ridges/km)
Beaufort and Chukchi Seas (combined)	Feb and Apr 1976	6.730	1.662	0.602	4.4
Blue Fox-Snow Bird leg of AIDJEX triangle	Feb 1976	5.483	1.566	0.639	2.6
Shear zone ($\mu \geq 6$ ridges/km) Beaufort and Chukchi Seas	Feb and Apr 1976	7.656	1.722	0.581	8.7
Beaufort Sea	Dec 1976	102.798	3.583	0.279	1.4
Barrow (Chukchi Sea)	Aug 1976	47.970	2.980	0.336	2.7
Beaufort Sea (Mackenzie Delta region, see Wadhams 1976)	Summer 1974 and Apr 1975	7.727	1.603	0.624	

To estimate the maximum ridge height expected along a specified length L of sampling track $P_c(h)$ is first calculated from

$$P(h) = 1/(\mu L).$$

Then the value of h corresponding to the specified value of $P_c(h)$ is obtained from the most appropriate curve in Figure 11. For instance, if the combined Beaufort and Chukchi curve is believed to be applicable, there are on the average 5.5 ridges/km, and if 1000 km of the ice is to be sampled, one would expect to find one ridge with a sail height equal to or greater than 6.0 m in the sample.

Extreme values

The problem with the previous approach is that it presupposes that the pertinent distribution function is known. As we have discussed for pressure ridge sails this is still a matter of some debate. Also, even if the form of the distribution function is known, there may be appreciable differences in the probabilities estimated from the tails of the same distribution fitted to different samples drawn from the same population.

To avoid these problems an alternate approach that is common in hydrology in studies of rare events such as floods can be utilized (Chow 1964). In hydrology, the data are usually time series, and the largest event in each of a sequence of specified fixed time intervals (e.g. the highest stream flow in each of a set of years) is used to generate the distribution of rare events. In the present case the basic data set is a space series and the largest ridge from each 20-km sampling interval will be used. Each ridge height value in this distribution of extreme height is then plotted using the Weibull plotting formula

$$T = 1/[P(X \geq x)] = (N+1)/M \qquad (11)$$

where T = the recurrence interval in terms of 20-km sampling units
$P(X \geq x)$ = the probability that X equals or exceeds some specified value x
N = the total number of values in the extreme height distribution
M = the order number of the items arranged in descending magnitude (i.e. $M = 1$ for the largest ridge).

It was found that when the data were displayed on normal probability paper the resulting plot was linear over the complete range of the observed data. Our results are in agreement with the conclusions of Slack et al. (1975) who found, based on a series of Monte Carlo simulations, that the normal distribution usually represented the distribution of extreme events better than

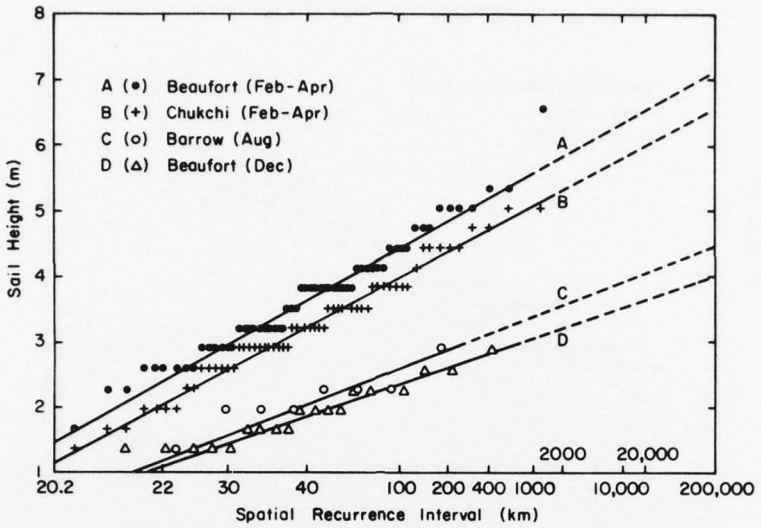

Figure 12. Ridge sail heights versus spatial recurrence intervals.

the Gumbel, log-normal or Weibull distributions.

Figure 12 shows the plots of the ridge height data. In this presentation we have again combined the February and April data inasmuch as the ice conditions would be expected to be similar. However, we have treated the Chukchi Sea observations separately from the Beaufort Sea observations. We have also replaced the recurrence interval expressed in terms of the total number of kilometers of laser track in the sample. As can be seen, the ridges in the Beaufort Sea run about 0.5 m higher than in the Chukchi Sea for similar spatial recurrence intervals. We have also plotted the results from Barrow in August and from the Beaufort Sea in December. Both of these data sets show appreciably lower ridge heights for similar spatial recurrence intervals. The March 1978 traverse out from Cross Island, although not shown, gives a straight line similar to the line shown for February–April in the Chukchi Sea. The largest ridge obtained in our traverses (6.55 m) would appear to be quite a rare event in that one such ridge would, on the average, be expected every 20,000 km if its spatial return period is obtained from a linear extrapolation of the remainder of the data in the February–April sample distribution for the Beaufort Sea.

If we now use curve A in Figure 12, we find that, if 1000 km of ice in the Beaufort Sea were sampled during the February–April time period,we would expect the sample to contain 1 ridge with a sail height equal to or greater than 5.6 m. Note that this value is 0.4 m lower than the estimate (6.0 m) made by using the tail of the Wadhams distribution.

In addition to constructing extreme value plots from the actual data, the Hibler and Wadhams models were also used to generate samples of extreme ridge heights. By using the $\bar{h}$ and μ values actually found in the February and April Beaufort Sea tracks, sample distributions were generated using a simple Monte Carlo simulation. The largest ridge from each spatial sample interval was plotted as previously described and the results from each of the two models plus the Beaufort Sea February–April curve are shown in Figure 13. The data are not as linear as the extreme value plots from the original data. Note again that the extreme values from the Wadhams model predict larger ridges at the longer recurrence intervals than does the extreme value plot from the original data (the straight line). The highest ridge generated by the Wadhams model was 6.65 m, nearly the same as that found in the actual data. (The data plotted are the generated ridge heights assigned to the class interval in which they fall.)

Applications to offshore design

Persons interested in the design of offshore structures for arctic areas such as the Beaufort

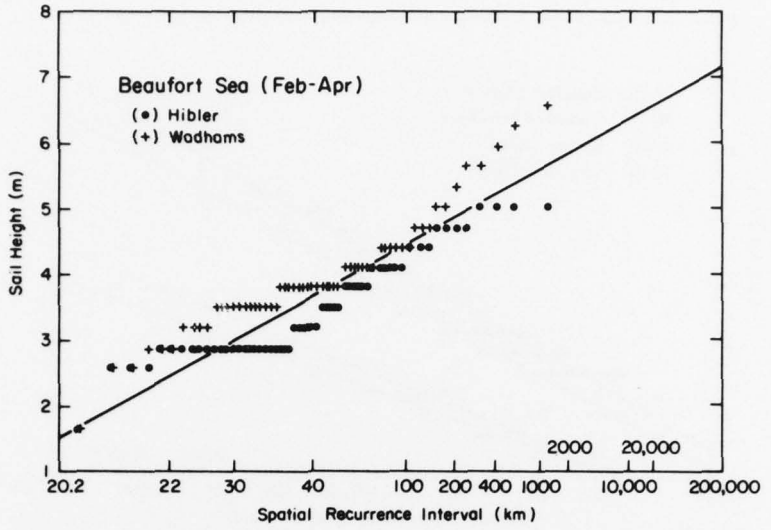

Figure 13. Monte Carlo simulation of the extreme ridge heights generated by the Wadhams and Hibler models using μ and $\bar{h}$ from the Beaufort Sea February and April tracks. The straight line is that obtained from the actual data.

Sea are, of course, not interested in spatial recurrence intervals but in temporal recurrence intervals, the average interval of time within which an event of magnitude x will be equaled or exceeded once. Offshore structures are essentially immobile while engaged in exploration and production activities. Therefore, they must take the ice as it comes. To convert spatial to temporal recurrence intervals, one must know how much ice drifts past a specified fixed point during a given period of time.

Ice drift velocities far from the coast are far from satisfactorily known. Even so, values exist upon which rough estimates can be made. For instance, we could use 2.5 km/day (900 km/yr) based on the observations made during AIDJEX (Thorndike and Colony 1978). If we are interested in the 100-year event, this corresponds to 91,250 km of ice drifting over a site. Using μ = 2.6 ridges/km and assuming that the AIDJEX curve holds for the entire year, we obtain an estimated sail height of 8.7 m from the Wadhams distribution. In a similar manner the 10-year sail height is estimated to be 7.3 m, only slightly lower.

At sites closer to the coast but still always within the pack ice zone, drift velocity observations are more limited. Probably the best estimates come from recent buoy deployments which have indicated ice drifts averaging roughly 0.7 km/day in the winter and 3.3 km/day in the summer (Shapiro et al. 1978). Assuming three months of summer and nine months of winter, we have approximately 300 km of summer drift and 200 km of winter drift each year. Using μ = 5.5 ridges/km in the winter and 2.7 ridges/km in the summer, we obtain 1100 winter ridges and 810 summer ridges each year resulting in estimates of 7.8 m for the 100-year winter ridge and 4.7 m for the 100-year summer ridge. Considering the fact that the ice in the summer is much warmer and has an appreciably lower strength than the ice in the winter (Schwarz and Weeks 1977), it is the winter ridge that is clearly of concern. The 100-year ridge sail based on the extreme value plot is 6.6 m (winter) and 4.2 m (summer)—significantly lower values.

In shallower (<20-m) near-shore but still unprotected areas, the ice becomes essentially immobile during the winter and late spring (Weeks

et al. 1977, Tucker et al. 1979). Taking ice movements to be 0.7 km/day during November, December and June, 0.2 km/day during January through May, and 3.3 km/day during July through October gives rough estimates of 100 km of winter drift and 400 km of summer drift. Using the same μ values as before gives 550 winter ridges/year and 1080 summer ridges/year. The 100-year winter and summer ridge sail heights would be estimated from the Wadhams distribution as 6.5 m and 4.8 m (6.3 and 4.2 m from the extreme value plot). Again it is the winter ridge that is important even though more summer ridges are encountered. Assuming a keel draft/sail height ratio of 4:1 results in an estimated 100-year ridge thickness of 32.5 m. Inasmuch as we are considering water depths of <20 m, the design ridge at a given site would undoubtedly be presumed to have a thickness equal to the water depth plus an appropriate freeboard.

Finally within the protected waters of the lagoon systems between the barrier islands and the mainland, another ice movement scenario would be expected to hold. Here the total winter ice motion is a few hundred meters, the summer period is essentially ice free, the majority of the ice movement occurs during the freezeup and breakup, and the number of ridges/km is low. Our data poorly characterize this region as our sampling tracks were largely outside of the barrier islands. Because the water is commonly quite shallow (maximum depth of 7.6 m), the design ridge would probably again be assumed to be equal to the water depth plus an appropriate freeboard.

We suggest that the above discussion be read with a considerable "pinch of salt" inasmuch as we have utilized a one-year space series to make projections about a 100-year time series. This should be all right if the number of ridges per kilometer remains relatively constant from year to year. This, of course, can only be verified by further sampling. However, we do think that the discussion was useful in that it has clarified two points. These are:

1. Ridge sail height observations such as reported here are directly useful in assessing encounter probabilities between offshore structures and ridges of different heights.

2. Values for design ridges will be highly dependent on the local environment conditions, specifically the seasonal nature of the local ridge height distributions, the long-term characteristics of the ice drift at the site, and the water depth.

CONCLUSIONS

Laser profilometer data collected during February, April, August, and December 1976 and March 1978 suggest the following conclusions regarding the nature of pressure ridge sails occurring over the continental shelves of the Chukchi and Beaufort Seas.

1. There is a systematic seasonal variation in mean sail height $\bar{h}$ measured relative to a lower cutoff of 0.9 m (3 ft) with values being low (1.1 to 1.2 m) in the summer (August) and early winter (December) and increasing appreciably by late winter (February–April) to values as high as 1.8 m.

2. At any given time there is no systematic spatial variation in $\bar{h}$.

3. The number of ridges per kilometer (μ) is smaller in the summer and early winter (2.7 in August based on a sample at Barrow only and 1.4 in December) and increases substantially in February and April (4.4 and 4.5, respectively).

4. In February and April μ values in the Beaufort Sea were slightly higher than in the Chukchi Sea. The most heavily ridged track was off Barter Island followed by the Cross Island track.

5. In general, largest μ values occur 20 to 60 km off the coast.

6. Patterns shown by variations in the ridging intensity (I_r) are similar to those shown by the variations in μ

7. The Wadhams model for ridge frequency gives better agreement with observed ridge height distributions, particularly in the higher ridge categories, than does the Hibler distribution.

8. The distributions of largest ridges per 20 km are shown to be nearly normal and can be used to estimate the spatial recurrence intervals of large pressure ridges.

9. To obtain good estimates of the temporal recurrence intervals of large ridges, good estimates must be available of the average drift of sea ice in the near-coastal areas of interest. Unfortunately, such information is at present quite limited.

10. Estimates of the sail heights that correspond to given spatial recurrence intervals are higher when based on the tail of the Wadhams distribution than when based on an extreme value approach.

It should be stressed that the observational data upon which these conclusions are based are far from adequate either spatially or temporally to delineate ridging patterns along the North Slope of Alaska. Therefore, the above conclusions should be viewed with appropriate skepticism until verified by additional data.

LITERATURE CITED

Chow, V.T. (1964) Statistical and probability analysis of hydrologic data. Part I: Frequency analysis. In *Handbook of Applied Hydrology* (V.T. Chow, ed.). New York: McGraw-Hill, p. 8-1 to 8-42.

Dunbar, M. and W. Wittman (1962) Some features of ice movement in the Arctic Basin. In *Proceedings of the Arctic Basin Symposium*, Arctic Institute of North America, Calgary, Alberta, p. 90-108.

Gonin, G.B. (1960) Calculation of the hummockiness of ice by statistical treatment of air photographic data (in Russian). *Problemy Arktiki i Antarktiki*, vol. 3, p. 93-100.

Hibler, W.D. III, (1978) Model simulation of nearshore ice drift, deformation, and thicknesses. In *POAC 77, Proceedings of the Fourth International Conference on Port and Ocean Engineering under Arctic Conditions*, (D.G. Muggeridge, ed.) Memorial University, St. Johns, Newfoundland, Canada, vol. I, p. 33-44.

Hibler, W.D. III and S.F. Ackley (1973) A sea ice terrain model and its application to surface vehicle trafficability. CRREL Research Report 314, AD 774195.

Hibler, W.D. III, W.F. Weeks, and S.J. Mock (1972) Statistical aspects of sea ice ridge distributions. *Journal of Geophysical Research*, vol. 77, p. 5954-70.

Hibler, W.D. III, S.J. Mock, and W.B. Tucker III (1974) Classification and variation of sea ice ridging in the Western Arctic Basin. *Journal of Geophysical Research*, vol. 79, p. 2735-43.

Ketchum, R.D. Jr. (1971) Airborne laser profiling of the Arctic pack ice. *Remote Sensing of the Environment*, vol. 2, p. 41-52.

Kovacs, A. and M. Mellor (1974) Sea ice morphology as a geologic agent in the southern Beaufort Sea. In *The Coast and Shelf of the Beaufort Sea*. (J.C. Reed and J.E. Sater eds.) Arctic Institute of North America, Arlington, Virginia, p. 113-161.

Lowry, R.T. (1975) An experiment in ice profiling in Nares Strait and the Arctic Ocean. *Journal of Glaciology*, vol. 15, p. 462-3.

Parmerter, R.R. and M.D. Coon (1972) A model of pressure ridge formation in sea ice. *Journal of Geophysical Research*, vol. 77, p. 6565-75.

Pritchard, R.S. (1978) A simulation of nearshore winter ice dynamics in the Beaufort Sea. In *Sea Ice Processes and Models. Proceedings of the AIDJEX/ICSI Symposium* (R.S. Pritchard, ed.), University of Washington Press, Seattle.

Reimnitz, E., L. Toimil and P. Barnes (1978) Arctic continental shelf morphology related to sea-ice zonation, Beaufort Sea, Alaska. *Marine Geology*, vol. 28, p. 179-210.

Slack, J.R., J.R. Wallis, and N.C. Matalas (1975) On the value of information to flood frequency analysis. *Water Resources Research*, vol. 11, p. 629-47.

Thorndike, A.S. and R. Colony (1978) Large-scale ice motion in the Beaufort Sea during AIDJEX, April 1975-April 1976. *Sea Ice Processes and Models, Proceedings of the AIDJEX/ICSI Symposium* (R.S. Pritchard, ed.). University of Washington Press, Seattle.

Tooma, S.G. and W.B. Tucker III (1973) Statistical comparison of airborne laser and stereophotogrammetric sea ice profiles. *Remote Sensing of Environment*, vol. 2, p. 261-72.

Tucker, W.B. III and V.H. Westhall (1973) Arctic sea ice ridge frequency distribution derived from laser profiles. *AIDJEX Bulletin No. 21*, p. 171-180.

Tucker, W.B. III, W.F. Weeks, A. Kovacs, and A.J. Gow (1978) Nearshore ice motion at Prudhoe Bay, Alaska. In *Sea Ice Processes and Models, Proceedings of the AIDJEX/ICSI Symposium* (R.S. Pritchard, ed.), University of Washington Press, Seattle.

Wadhams, P. (1976) Sea ice topography in the Beaufort Sea and its effect on oil containment. *AIDJEX Bulletin No. 33*, p. 1-52.

Wadhams, P. (1978) A comparison of sonar and laser profiles along corresponding tracks in the Arctic Ocean. In *Sea Ice Processes and Models, Proceedings of the AIDJEX/ICSI Symposium* (R.S. Pritchard, ed.), University of Washington Press, Seattle.

Wadhams, P. and R.J. Horne (1978) An analysis of ice profiles obtained by submarine sonar in the AIDJEX area of the Beaufort Sea. *Scott Polar Research Institute Technical Report 78-1*.

Weeks, W.F., A. Kovacs and W.D. Hibler (1971) Pressure ridge characteristics in the arctic coastal environment. *Proceedings, First International Conference on Port and Ocean Engineering Under Arctic Conditions*, vol. I, p. 152-183. Technical University of Norway, Trondheim.

Weeks, W.F., A. Kovacs, S.J. Mock, W.F. Hibler III and A.J. Gow (1977) Studies of the movement of coastal sea ice near Prudhoe Bay, Alaska. *Journal of Glaciology*, vol. 19, p. 533-546.

Weeks, W.F., W.B. Tucker III, M. Frank and S.Fungcharoen (1978) Characterization of surface roughness and floe geometry of the sea ice over the continental shelves of the Beaufort and Chukchi Seas. In *Sea Ice Processes and Models, Proceedings of the AIDJEX/ICSISymposium* (R.S. Pritchard, ed.), University of Washington Press, Seattle.

APPENDIX A. TABULATED ICE RIDGE DATA.

Table A1. Tabulated data on the frequency distributions of ridge heights as a function of location and time of year.

The numbers in the body of the table give the number of ridges counted.

Distance from shore (km)	Heights of ridge sails (Midpoints of class intervals) 1.07 (3.5)	1.37 (4.5)	1.67 (5.5)	1.98 (6.5)	2.28 (7.5)	2.59 (8.5)	2.90 (9.5)	3.20 (10.5)	3.50 (11.5)	3.81 (12.5)	4.11 (13.5)	4.42 (14.5)	4.72 (15.5)	5.03 (16.5)	5.33 (17.5) (m) (ft)
February 1976															
Point Lay															
180-200	37	23	14	16	7	6	2								
160-180	32	12	9	6	1				1						
140-160	29	18	18	8	3	2									
120-140	24	26	13	8	6	1	3								
100-120	22	20	16	11	8	2	1			1					
80-100	37	18	20	12	2	2	1	1		1					
60-80	54	38	23	12	12	5	1								
40-60	46	41	18	22	9	9	4	3	1						
20-40	25	14	12	5	4		2		1						
0-20	9	5		2											
Wainwright															
180-200	15	14	8	6	5	1	1	2	1						
160-180	10	5	5	3	1		2		1						
140-160	27	14	12	9	9	1	1	2							
120-140	23	19	8	5	6		2		2			1	1		
100-120	19	15	17	4	2	4	5			1					
80-100	20	14	13	11	6	3	1								
60-80	24	15	23	11	9	3		1							
40-60	28	17	19	12	6	2	3	1	1					1	
20-40	21	17	10	7	3	3	2		1						
0-20	15	15	9	8	6	4		1							
Barrow															
180-200	21	18	17	6	4	2									
160-180	15	9	7	8	4	2	3				1				
140-160	25	15	12	3	4	5	3	1				1			
120-140	17	13	9	9	6	8	4	2							
100-120	24	10	11	9	8	1						1			
80-100	20	10	4	4	4	3	1	1	1	1					
60-80	13	14	12	7	2	2	2		2	1	1			1	
40-60	14	21	14	4	13	1	2	1		3		1			
20-40	17	24	11	7	9	2	3		1	1	1		1		
0-20	17	14	11	4	1	4	4		1						
Lonely															
180-200	10	8	7	3	1	1									
160-180	35	22	5	3	3		3				1				
140-160	22	14	10	7	1	4	1	1	1						
120-140	18	16	7	7	4	3									
100-120	21	18	9	7	2		1	1							
80-100	28	17	18	10	3		2	4	1	1	1				
60-80	38	34	20	16	11	5	5	5		1					
40-60	36	30	29	20	14	5	3	2	1			1			
20-40	34	29	16	13	2	4		1	1						
0-20	1	1	1												
Cross Island															
180-200	21	9	9	6	2	2		1						1	
160-180	29	13	16	5	7	2		1							
140-160	13	7	8	7	2		2	2		1				1	
120-140	22	13	8	1	4	2	1								
100-120	35	25	21	11	6	5	6	1		1					
80-100	39	21	13	15	9	3	4	2	1	1	1		1		
60-80	58	40	24	15	14	10	1	3							

Table A1 (cont'd).

Distance from shore (km)	Heights of ridge sails (Midpoints of class intervals) 1.07 (3.5)	1.37 (4.5)	1.67 (5.5)	1.98 (6.5)	2.28 (7.5)	2.59 (8.5)	2.90 (9.5)	3.20 (10.5)	3.50 (11.5)	3.81 (12.5)	4.11 (13.5)	4.42 (14.5)	4.72 (15.5)	5.03 (16.5)	5.33 (17.5)	(m) (ft)
Cross Island (cont'd)																
40-60	69	38	33	17	8	6		2	1		1					
20-40	52	38	38	13	20	5	3	3	1	1	1		1		1	
0-20	25	21	7	7	1	2					1					
*Barter Island**																
180-200	16	18	13	5	6	3	4	1		1						
160-180	32	22	12	6	5	4	1	1			1					
140-160	25	23	5	4	2		1	1								
120-140	40	19	9	8	4	4	5	1		1						
100-120	45	29	11	10	7	6	4						1			
80-100	50	27	20	14	5	6	1	1	1		1			1		
60-80	34	27	20	10	8	6	3	1	1							
40-60	89	63	29	18	12	11	4	2	3	2	2	2				
20-40	96	56	43	34	16	9	6	5	1	1	1		1			
0-20	48	35	21	7	12	6	3	3	3	1		1				
April 1976																
Point Lay																
180-200	25	10	3	2	0											
160-180	34	10	1	0	0											
140-160	33	11	1	1	1											
120-140	35	12	4	0	0											
100-120	35	11	2	3	0											
80-100	35	15	5	1	0											
60-80	56	28	15	9	3	1										
40-60	35	17	21	8	3	1	2									
20-40	3	1	0	0	0											
0-20	7	5	3	1	0			1								
Wainwright																
180-200	48	22	8	8	6	3	0			1						
160-180	25	15	8	3	4	2	3		1							
140-160	28	13	8	1	1	1										
120-140	35	17	10	5	1	2	1	1								
100-120	33	21	4	4	1	0										
80-100	29	16	5	7	6	1	1									
60-80	32	30	16	8	4	0	1									
40-60	42	27	20	5	5	3	3	2								
20-40	36	28	9	7	3	3										
0-20	11	9	8	3	3	0		1								
Barrow																
180-200	31	12	12	8	4	1	1									
160-180	28	16	10	6		1	1									
140-160	31	14	2	5	6	1										
120-140	28	14	14	2	1	1	1									
100-120	14	14	12	5		1	2	1								
80-100	18	15	5	9	3	2	1	2	2							
60-80	26	10	9	2	1			1	1			1				
40-60	15	14	8	7	6	2	1			1						
20-40	24	20	7	2	4	5		2	2			1				
0-20	20	15	9	8	5	2			1	1						
Lonely																
180-200	30	27	10	4	4		1									
160-180	22	12	10	10	4	3	2	1								
140-160	45	18	10	6	3	2	1									
120-140	31	9	4	4	3	1	1									
100-120	39	21	16	13	6	2	5	1	1			1				

*One ridge sail 100 km from shore measured 6.40 m.

Table AI (cont'd).

Distance from shore (km)	Heights of ridge sails (Midpoints of class intervals) 1.07 (3.5)	1.37 (4.5)	1.67 (5.5)	1.98 (6.5)	2.28 (7.5)	2.59 (8.5)	2.90 (9.5)	3.20 (10.5)	3.50 (11.5)	3.81 (12.5)	4.11 (13.5)	4.42 (14.5)	4.72 (15.5)	5.03 (16.5)	5.33 (17.5) (m) (ft)
Lonely (cont'd)															
80-100	32	22	21	8	9	4	3	1		1					
60-80	44	44	31	19	13	10	2	1					1		
40-60	36	26	14	13	9	4	3		1	1					
20-40	39	42	14	9	14	6	1			1					1
0-20	27	14	5	4	1										
Cross Island															
180-200	33	3	6	2			1								
160-180	38	20	8	1	5	2									
140-160	35	22	10	4	2	3									
120-140	35	16	6	4	5	2									
100-120	41	24	13	5	5	2				1					
80-100	71	33	13	8	4	4	1			1					
60-80	63	55	22	7	6	5	1	2		1					
40-60	61	49	27	18	5	10		1		1				1	
20-40	101	58	34	18	8	7	2	1							
0-20	53	34	21	3	3	2	2	4							
Barter Island															
180-200	15	10	11	4	3	3		1							
160-180	22	23	10	4	3	5	1								
140-160	24	10	9	5	1										
120-140	33	32	11	6	3	1	1	1		2					
100-120	54	37	14	9	4	3	1	0		1	1				
80-100	66	53	34	17	6	9	3		1						
60-80	105	70	37	22	15	6	3	1							
40-60	125	65	42	14	9	6	3	2							
20-40	75	43	28	16	5	1		2		1					
0-20	66	55	35	6	2	1									
August 1976															
Barrow															
180-200	35	11	1	1											
160-180	31	17	3	4	2										
140-160	39	17	5	3	1										
120-140	50	22	9	4	4		1								
100-120	44	21	7	5											
80-100	34	11	6	3	1										
60-80	22	8	2	3											
40-60	10	1													
20-40															
0-20															
December 1976															
Point Lay															
180-200	31	8	4	5	1										
160-180	20	2			1										
140-160	13	7	5												
120-140	28	8	12	4											
100-120	10	2													
80-100	10	6	2	1											
60-80	12	3													
40-60															
20-40															
0-20	6	1	1												

Table A1 (cont'd).

Distance from shore (km)	Heights of ridge sails (Midpoints of class intervals) 1.07 m 3.5 ft	1.37 m 4.5 ft	1.67 m 5.5 ft	1.98 m 6.5 ft	2.28 m 7.5 ft	2.59 m 8.5 ft	2.90 m 9.5 ft	3.20 m 10.5 ft	3.50 m 11.5 ft	3.81 m 12.5 ft	4.11 m 13.5 ft	4.42 m 14.5 ft
Barrow												
180-200	2	1										
160-180	4	1										
140-160	1											
120-140	4			1								
100-120	20	2										
80-100	78	13	3	2	2							
60-80	55	9	3	1								
40-60	24	6	1									
20-40	51	4	1	1								
0-20	16	5										
Cross Island												
180-200	26	15	3	5		1						
160-180	9	5	3									
140-160	10	2	2	1								
120-140	5	2	1									
100-120	13	7	2	1								
80-100	7	2										
60-80	24	8	5		1							
40-60	22	11	2		1							
20-40	34	22	7	1	2							
0-20	36	14	9	2		1	1					
Barter Island												
180-200	9	7	2	1		1						
160-180	4	1										
140-160	4	1										
120-140	3	1										
100-120	3	2										
80-100	5	1	1									
60-80	11	11	2									
40-60	15	7	2	1								
20-40	30	14	5									
0-20	45	21	9	4	2							
March 1978												
Cross Island												
180-200												
160-180												
140-160	36	28	16	4	3	1	2					
120-140	13	9	2	3								
100-120	25	11	8	1	1		1					
80-100	21	3	3	1	1							
60-80	34	20	15	7	1	1	1					
40-60	44	22	13	4	7	2		2				
20-40	57	34	43	25	16	9	3	1	3			
0-20	57	61	42	24	22	16	6	3	3		4	1

Table AII. Values of mean ridge height ($\bar{h}$) measured above a lower cutoff of 0.9 m and the number of ridges/kilometer (μ) at different locations and times of the year (1976).

Distance from shore (km)	February						April						August	December			
	Point Lay	Wainwright	Barrow	Lonely	Cross Island	Barter Island	Point Lay	Wainwright	Barrow	Lonely	Cross Island	Barter Island	Barrow	Point Lay	Barrow	Cross Island	Barter Island
								$\bar{h}$ (m)									
180-200	1.56	1.65	1.49	1.47	1.56	1.69	1.31	1.42	1.45	1.39	1.25	1.57	1.17	1.28	1.17	1.32	1.35
160-180	1.37	1.61	1.69	1.41	1.50	1.53	1.15	1.53	1.39	1.60	1.35	1.51	1.30	1.15	1.13	1.26	1.13
140-160	1.46	1.58	1.62	1.57	1.78	1.40	1.20	1.31	1.39	1.37	1.37	1.36	1.26	1.27	1.07	1.25	1.13
120-140	1.53	1.64	1.78	1.52	1.45	1.55	1.19	1.40	1.38	1.37	1.38	1.47	1.32	1.33	1.25	1.22	1.14
100-120	1.60	1.65	1.58	1.47	1.62	1.58	1.21	1.28	1.55	1.59	1.41	1.43	1.26	1.12	1.09	1.25	1.18
80-100	1.50	1.60	1.63	1.65	1.68	1.55	1.22	1.45	1.66	1.60	1.37	1.50	1.26	1.27	1.17	1.13	1.29
60-80	1.48	1.61	1.79	1.66	1.56	1.60	1.34	1.43	1.49	1.61	1.44	1.45	1.25	1.13	1.15	1.24	1.26
40-60	1.62	1.65	1.79	1.67	1.50	1.58	1.46	1.49	1.63	1.59	1.52	1.40	1.09	1.18	1.15	1.23	1.24
20-40	1.50	1.53	1.74	1.50	1.67	1.59	1.14	1.40	1.62	1.58	1.33	1.41			1.12	1.28	1.22
0-20	1.28	1.66	1.63	1.37	1.45	1.63	1.44	1.53	1.58	1.30	1.32	1.36			1.14	1.30	1.29
Average	1.49	1.62	1.67	1.52	1.58	1.57	1.27	1.42	1.51	1.50	1.37	1.45	1.23	1.22	1.14	1.25	1.22
Monthly average			1.58						1.42						1.21		
								μ (ridges/km)									
180-200	5.25	2.65	3.40	1.50	2.55	3.35	2.10	4.80	3.45	3.80	2.25	2.35	2.40	2.45	0.15	2.50	1.00
160-180	3.05	1.35	2.45	3.60	3.65	4.20	2.25	3.05	3.10	3.20	3.70	3.40	2.85	1.15	0.25	0.85	0.25
140-160	3.90	3.75	3.45	3.05	2.15	3.05	2.35	2.60	2.95	4.25	3.80	2.45	3.25	1.25	0.05	0.75	0.25
120-140	4.05	3.35	3.40	2.75	2.55	4.55	2.55	3.60	3.05	2.65	3.40	4.50	4.50	2.60	0.25	0.40	0.20
100-120	4.05	3.35	3.20	2.95	5.55	5.70	2.55	3.15	2.45	5.25	4.55	6.20	3.85	0.60	1.10	1.15	0.25
80-100	4.70	3.40	2.45	4.25	5.50	6.35	2.80	3.25	2.85	5.05	6.75	9.45	2.75	0.95	4.90	0.45	0.40
60-80	7.25	4.30	2.85	6.75	8.25	5.50	5.60	4.55	2.65	8.25	8.10	12.95	1.75	0.75	3.40	1.90	1.20
40-60	7.65	4.50	3.70	7.05	8.75	11.85	4.35	5.35	2.70	5.35	8.65	13.30	0.55	0.40	1.55	1.80	1.25
20-40	3.15	3.15	3.85	5.00	8.85	13.45	0.20	4.30	3.35	6.35	11.70	8.55			2.85	3.30	2.45
0-20	0.80	2.95	2.80	0.15	3.20	7.00	0.85	1.75	3.05	2.55	6.60	8.25			1.05	3.15	4.05
Average	4.38	3.28	3.16	3.70	5.10	6.50	2.56	3.64	2.96	4.67	5.95	7.14	2.73	1.27	1.56	1.63	1.13
Monthly average			4.35						4.49						1.40		

Table AIII. Tabulation of the constants for the Wadhams (α, β) and Hibler (N_0, λ) ridge height distributions determined from the data presented in Table A1.

Distance from shore (km)	February 1976						April 1976						August 1976	December 1976				March 1978
	Point Lay	Wainwright	Barrow	Lonely	Cross Island	Barter Island	Point Lay	Wainwright	Barrow	Lonely	Cross Island	Barter Island	Barrow	Point Lay	Barrow	Cross Island	Barter Island	Cross Island
								α (km-m)$^{-1}$										
180-200	10.32	3.83	8.50	4.20	4.91	4.23	15.85	18.05	10.76	16.48	31.28	4.36	105.40	23.87	6.58	18.38	5.46	
160-180	15.53	2.21	3.09	14.04	8.85	9.27	146.89	6.76	13.89	5.39	20.97	8.21	24.84	77.94	25.95	10.13	25.95	
140-160	11.78	6.81	5.46	5.79	2.20	12.84	64.92	20.71	13.16	21.43	18.24	13.12	42.91	13.46	40.34	10.43	25.95	17.63
120-140	8.87	5.03	3.41	6.23	8.03	9.35	82.50	14.74	14.08	13.56	15.81	12.61	32.90	17.94	3.48	8.03	14.55	10.05
100-120	6.81	4.82	5.86	8.40	8.79	10.21	57.79	30.68	5.03	9.01	17.19	21.52	45.56	81.02	298.35	15.5	7.79	16.02
80-100	11.59	5.82	3.71	6.15	7.30	12.64	56.23	10.13	4.03	8.41	33.75	23.71	32.02	10.10	211.21	39.68	3.53	23.89
60-80	19.22	7.12	2.76	9.27	16.17	9.32	33.29	15.97	6.79	13.29	26.84	40.78	24.33	77.84	224.78	28.39	15.35	16.43
40-60	12.31	6.54	3.68	9.48	21.66	20.86	13.04	13.79	4.11	9.31	19.88	55.55	149.15		106.99	32.44	19.99	16.37
20-40	7.90	6.72	4.30	12.26	11.99	23.37	14.56	17.75	5.26	11.67	16.57	32.46			414.07	32.35	51.28	14.59
0-20	8.43	4.04	4.24	0.74	10.15	10.68	2.75	3.85	5.39	20.53	18.27	45.48		14.09	82.85	25.79	37.91	13.84
								β (m^{-1})										
180-200	1.55	1.36	1.71	1.79	1.54	1.28	2.51	1.99	1.86	2.09	2.98	1.52	3.93	2.70	3.65	2.49	2.26	
160-280	2.21	1.44	1.28	2.02	1.69	1.63	4.27	1.63	1.63	1.46	2.73	1.69	2.61	4.31	4.69	2.86	4.69	
140-160	1.84	1.51	1.42	1.53	1.16	2.07	3.54	2.55	2.12	2.20	2.17	2.25	2.94	2.78	6.56	2.98	4.69	2.02
120-140	1.62	1.39	1.15	1.65	1.87	1.58	3.68	2.05	2.14	2.21	2.14	1.79	2.48	2.44	2.98	3.28	4.37	2.49
100-120	1.46	1.36	1.51	1.80	1.42	1.49	3.38	2.70	1.58	1.47	1.99	1.93	2.85	4.92	5.55	2.96	3.64	2.43
80-100	1.70	1.47	1.39	1.36	1.31	1.56	3.28	1.86	1.35	1.45	2.19	1.72	2.84	2.77	3.92	4.54	2.62	3.12
60-80	1.75	1.45	1.13	1.33	1.55	1.46	2.33	1.95	1.73	1.43	1.74	1.87	2.98	4.69	4.29	3.04	2.92	2.06
40-60	1.42	1.37	1.15	1.32	1.71	1.49	1.83	1.73	1.39	1.48	1.66	2.07	5.55		4.32	3.19	3.09	1.94
20-40	1.72	1.61	1.21	1.69	1.32	1.48	4.37	2.06	1.41	1.51	1.95	2.00			4.99	2.71	3.31	1.39
0-20	2.76	1.33	1.39	2.18	1.87	1.39	1.89	1.63	1.49	2.56	1.78	2.27		3.75	4.44	2.57	2.67	1.23
								N_0 (km-m)$^{-1}$										
180-200	2.67	1.10	2.04	0.96	1.28	1.27	2.51	3.72	2.37	3.22	3.91	1.16	8.21	3.42	0.52	2.95	0.98	
160-180	2.86	0.61	0.93	2.85	2.14	2.31	9.68	1.68	2.69	1.47	3.71	1.98	3.73	5.06	1.41	1.35	1.41	
140-160	2.63	1.82	1.52	1.52	0.71	2.54	6.13	3.22	2.55	3.96	3.44	2.37	5.46	1.86	0.88	1.30	1.41	3.58
120-140	2.22	1.43	1.10	1.54	1.77	2.39	7.30	2.94	2.69	2.49	3.01	2.89	5.28	2.94	0.44	0.87	0.92	1.60
100-120	1.87	1.39	1.56	1.92	2.45	2.73	5.93	4.41	1.29	2.45	3.54	4.56	6.06	3.90	10.61	1.96	0.70	2.65
80-100	2.78	1.58	1.05	1.77	2.16	3.26	6.05	2.24	1.17	2.31	6.26	5.61	4.29	1.40	16.57	2.30	0.53	2.79
60-80	4.49	1.96	1.90	2.71	4.19	2.54	5.78	3.38	1.61	3.68	5.79	8.96	3.04	4.21	14.74	3.44	1.98	3.26
40-60	3.38	1.86	1.19	2.79	5.18	5.61	2.91	3.26	1.16	2.52	4.88	11.01	5.31		6.89	3.65	2.36	3.47
20-40	1.88	1.69	1.34	2.95	3.52	6.31	0.92	3.54	1.47	3.09	8.74	6.67			19.36	4.64	5.43	4.12
0-20	1.18	1.18	1.20	0.14	2.23	3.01	0.60	0.96	1.45	3.18	4.21	8.13		1.21	5.09	3.97	5.53	4.27
								λ (m^{-2})										
180-200	0.39	0.31	0.45	0.47	0.38	0.29	0.77	0.56	0.51	0.60	0.99	0.37	1.44	0.86	1.44	0.78	0.68	
160-180	0.66	0.34	0.29	0.57	0.44	0.42	1.60	0.42	0.61	0.36	0.69	0.44	0.83	1.63	1.81	0.94	1.81	
140-160	0.49	0.37	0.34	0.38	0.25	0.59	1.25	0.79	0.61	0.65	0.64	0.67	0.97	0.90	2.73	0.99	1.81	0.57
120-140	0.42	0.32	0.25	0.42	0.51	0.39	1.21	0.58	0.62	0.66	0.57	0.47	0.76	0.75	0.99	1.13	1.66	0.77
100-120	0.36	0.31	0.37	0.48	0.33	0.37	1.17	0.86	0.39	0.36	0.56	0.54	0.94	1.92	2.23	0.98	1.30	0.74
80-100	0.44	0.35	0.32	0.31	0.30	0.39	1.13	0.51	0.31	0.34	0.65	0.45	0.92	0.89	1.43	1.73	0.83	1.05
60-80	0.46	0.34	0.24	0.30	0.39	0.36	0.70	0.53	0.45	0.34	0.53	0.51	0.99	1.81	1.61	1.02	0.96	0.59
40-60	0.33	0.32	0.24	0.30	0.44	0.37	0.49	0.45	0.33	0.36	0.43	0.59	2.23		1.63	1.09	1.04	0.54
20-40	0.45	0.41	0.24	0.44	0.30	0.35	1.66	0.59	0.33	0.38	0.55	0.56			1.95	0.87	1.14	0.33
0-20	0.89	0.30	0.26	0.65	0.51	0.33	0.52	0.42	0.36	0.79	0.47	0.68		1.34	1.69	0.81	0.85	0.27

A facsimile catalog card in Library of Congress MARC format is reproduced below.

Tucker, W.B., III
Sea ice ridging over the Alaskan continental shelf / by W.B. Tucker, III, W.F. Weeks and M.D. Frank. Hanover, N.H.: U.S. Cold Regions Research and Engineering Laboratory; Springfield, Va.: available from National Technical Information Service, 1978.
iv, 28 p., illus.; 27 cm. (CRREL Report 79-8.)
Prepared for National Oceanic and Atmospheric Administration and Bureau of Land Management, by Corps of Engineers, U.S. Army Cold Regions Research and Engineering Laboratory.
Bibliography: p. 18.
1. Arctic Ocean. 2. Extreme values. 3. Laser profilometry. 4. Ridges. 5. Sea ice. 6. Statistical models. I. Weeks, W.F. II. Frank, M.D. III. United States. Army. Corps of Engineers. IV. Army Cold Regions Research and Engineering Laboratory, Hanover, N.H. V. Series: CRREL Report 79-8.

☆U.S. GOVERNMENT PRINTING OFFICE: 1979—601-409/57